

Article

## RPV Model Parameters Based on Hyperspectral Bidirectional Reflectance Measurements of *Fagus sylvatica* L. Leaves

Dimitrios Biliouris<sup>1,\*</sup>, Dimitry van der Zande<sup>1</sup>, Willem W. Verstraeten<sup>1</sup>, Jan Stuckens<sup>1</sup>, Bart Muys<sup>2</sup>, Philip Dutré<sup>3</sup> and Pol Coppin<sup>1</sup>

<sup>1</sup> Department of Biosystems, Katholieke Universiteit Leuven, M3-BIORES, Willem de Croylaan 34, BE-3001 Leuven, Belgium

<sup>2</sup> Department of Earth and Environmental Sciences, Katholieke Universiteit Leuven, Celestijnenlaan 200 E, BE-3001 Leuven, Belgium

<sup>3</sup> Department of Computer Sciences, Katholieke Universiteit Leuven, Celestijnenlaan 200A, BE-3001 Leuven, Belgium

\* Author to whom correspondence should be addressed; E-Mail: Dimitrios.Biliouris@biw.kuleuven.be; Tel.: +32-16329739; Fax: +32-16329724

Received: 6 April 2009; in revised form: 31 May 2009 / Accepted: 10 June 2009 /

Published: 11 June 2009

---

**Abstract:** The bidirectional reflectance parametric and semi-empirical Rahman-Pinty-Verstraete (RPV) model was inverted based on Bidirectional Reflectance Factor (BRF) measurements of 60 *Fagus sylvatica* L. leaves in the optical domain between 400 nm and 2,500 nm. This was accomplished using data retrieved from the Compact Laboratory Spectro-Goniometer (CLabSpeG) with an azimuth and zenith angular step of 30 and 15 degrees, respectively. Wavelength depended RPV parameters describing the leaf reflectance shape ( $\rho_0$ ), the curve convexity ( $k$ ) and the dominant forward scattering ( $\Theta$ ) were derived using the RPV inversion-2 software (Joint Research Centre) package with Correlation Coefficient values between modelled and measured data varying between 0.71 and 0.99 for all wavelengths, azimuth and zenith positions. The RPV model parameters were compared with a set of leaves not participating in the inversion procedure and presented Correlation Coefficient values ranging between 0.64 and 0.94 suggesting that RPV could be also used for simulating single canopy elements such as leaves.

**Keywords:** BRF-measurement; goniometer; spectroradiometer; *Fagus sylvatica* L.; leaves; Rahman-Pinty-Verstraete reflectance model

---

## 1. Introduction

Interpreting remote sensing data while providing a link with physical vegetation properties depends on the understanding of the multitude of factors controlling canopy reflectance signals [1]. Previous research was conducted on comparing reflectance models for a variety of surface types and illumination – viewing scenarios to accurately simulate the Bidirectional Reflectance Distribution Function (BRDF) of a canopy [2,3]. Several BRDF parametric models have been developed guided by the physical expressions found in the forward modelling BRDF theories. Two mathematical forms of parametric models have been considered, namely additive and multiplicative [4]. The first are based on the kernel driven approach [5], while the latter are best represented by the semi-empirical three-parameter model of [6,7] that is commonly called the Rahman-Pinty-Verstraete (RPV) model. Several efforts have been made to validate and compare these models. The RADIATION transfer Model Intercomparison (RAMI) experiment is a notable example [8,9]. The RPV model returns Bidirectional Reflectance Factor (BRF) values for an arbitrary geophysical medium. It is able to describe the hot spot effect and has been tested both in forward and inverse mode against several datasets including field and laboratory data providing satisfactory results [2,6,7,10-12]. To date, the model was mainly used to simulate reflectance of non-flat canopy targets that present a backscattering behaviour, in contrast with single leaf characteristics. However, the spectral and directional scattering properties of leaves, which are spatially distributed inside a crown/canopy, and ground reflectance properties, are important factors contributing to the BRDF signal of a canopy target [13-15].

To the knowledge of the authors, documentation of hyperspectral variations of reflectance anisotropy effects at the leaf level is still very scarce. Considering the availability of global illumination algorithms in combination with the present opportunities to measure the BRDF of leaves, the potential of the RPV model to represent the BRDF of leaves in the 400-2,500 nm spectral range was investigated in this study. This RPV based BRDF can then be possible used as a simplified approximation input of directional reflectance for virtual stands representations, either for simulation, modelling or visualization purposes.

A Compact Laboratory Spectro-Goniometric device (CLabSpeG) [16] was used to measure the Bidirectional Reflectance Factor (BRF), of 12 sets of five *Fagus sylvatica* L. leaves each, for the wavelength range of 400 to 2,500 nm covering the hemisphere between nadir and 60°, with 30° and 15° angular steps in azimuth and zenith, respectively. This paper focuses on:

1. The inversion of the widely applied Rahman-Pinty-Verstraete (RPV) model based on eight Bidirectional Reflectance Factor (BRF) data sets of leaves in the 400 to 2,500 nm spectral range.
2. The evaluation of the retrieved RPV parameters based on four measured BRF data sets by comparison among modelled and measured leaf BRF values along the full hyperspectral dynamic range of the spectroradiometer.

## 2. Theoretical background: RPV model description

The RPV model is a semi-empirical parametric model [7,17] that can provide: (i) the shape of the BRDF as a lower boundary condition for atmospheric or vegetation models [18]; (ii) the hypothetical reflectance to a non measured angle of illumination and observation [19]; (iii) the estimated albedo of a surface by integrating the sample BRDF over all viewing angles [20]; and (iv) the identification of surface properties such as underlying vegetation structure and structural scattering index [21,22].

The model [7] is based on three parameters ( $\rho_0$ ,  $k$ ,  $\Theta$ ) [4,23] to express the reflectance  $\rho_s$  of a surface illuminated from direction  $(\theta_i, \phi_i)$  and observed from direction  $(\theta_r, \phi_r)$ . A Lambertian term ( $\rho_0$ ) describes the overall amplitude of the reflectance. The basic bowl shape of the BRDF, which is a function of view and solar zenith angle, is given by a modified Minnaert function [24] that involves power functions of the zenith angle cosines governed by the second parameter ( $k$ ). The third parameter ( $\Theta$ ) is used as input in a Henyey-Greenstein function in  $F(g)$  [25] that controls the relative amount of forward and backward scattering :

$$\rho_s(\theta_i, \phi_i; \theta_r, \phi_r; \lambda) = \rho_0 \cdot M(\theta_i, \theta_r, k) \cdot F(g) \cdot [1 + R(G)] \quad (1)$$

where  $\rho_0$  and  $k$  are two empirical surface parameters, and  $\Theta$  controls function  $F(g)$ .  $\rho_0$  characterizes the intensity of the reflectance of the surface and the albedo ( $0 \leq \rho_0 \leq 1$ ). The parameter  $k$  indicates the level of anisotropy of the surface where  $\Theta$  is the function parameter controlling the relative amount of forward ( $\Theta \geq 0$ ) and backward scattering ( $\Theta \leq 0$ ) [24]. Considering that leaf reflectance measurements obtained with the CLabSpeG, do not produce a hot spot effect, the value of  $\rho_0$  was set equal to one in equation 5. The components of the RPV model are given below (equations 2-6).

The Minnaert function is:

$$M(\theta_i, \theta_r, k) = (\cos \theta_i \cdot \cos \theta_r)^{k-1} \cdot (\cos \theta_i + \cos \theta_r)^{k-1} \quad (2)$$

The function  $F(g)$  is:

$$F(g) = \frac{1 - \Theta^2}{[1 + \Theta^2 + 2\Theta \cdot \cos g]^{1.5}} \quad (3)$$

The phase angle  $g$  is given by:

$$\cos g = \cos \theta_i \cdot \cos \theta_r + \sin \theta_i \cdot \sin \theta_r \cdot \cos(\phi_i - \phi_r) \quad (4)$$

The hot-spot effect is approximated by:

$$1 + R(G) = 1 + \frac{1 - \rho_0}{1 + G} \quad (5)$$

where  $G$  is the geometric factor given by:

$$G = [\tan^2 \theta_i + \tan^2 \theta_r - 2 \tan \theta_i \cdot \tan \theta_r \cdot \cos(\phi_i - \phi_r)]^{0.5} \quad (6)$$

### 3. Data description

In August 2006, branches of two 13 year old *Fagus sylvatica* L. trees were collected every morning and kept in water for a maximum period of two hours. This ensured a negligible time-span between the actual cutting of a leaf from the branch and the initiation of BRF measurements with the CLabSpeG goniometer in our laboratory. Branches were chosen from the outside and the top part of the trees. The leaves were placed on the sample holder horizontally inside the GLabSpeG goniometer with the adaxial side facing upwards, and the main axis orientation towards the 0° of the light source azimuth and the 90° of the sensor. This sample holder was covered with an absorptive black textile (oscuratinto colour 211, Création Baumann, Switzerland) that obtains near zero reflectance in the 400-2,500 nm range of the spectroradiometer to ensure that no reflectance contributions originate from the sample holder. The size of each sampled leaf was sufficiently large to make certain that the footprint of the sensor solely measured the sampled leaf, while the footprint of the light source was larger than the leaf. An ASD Field Spec Pro JR spectroradiometer with a field of view (FOV) of 1° was used to capture radiance readings with a footprint diameter of 0.025 m at nadir position and 0.05 m at 60°. The spectral resolution was 3 nm in the visible and 30 nm in the infrared, with an associated sampling interval of 1.4 nm for the 350-1,000 nm range and 2 nm for the 1,000-2,500 nm range. Moreover, data at the 0°/0° light/sensor position could not be retrieved due to shadow casting on the measured sample. Additional details about the measurement setup can be found in [16]. A set up of the measurements is given in Figure 1.

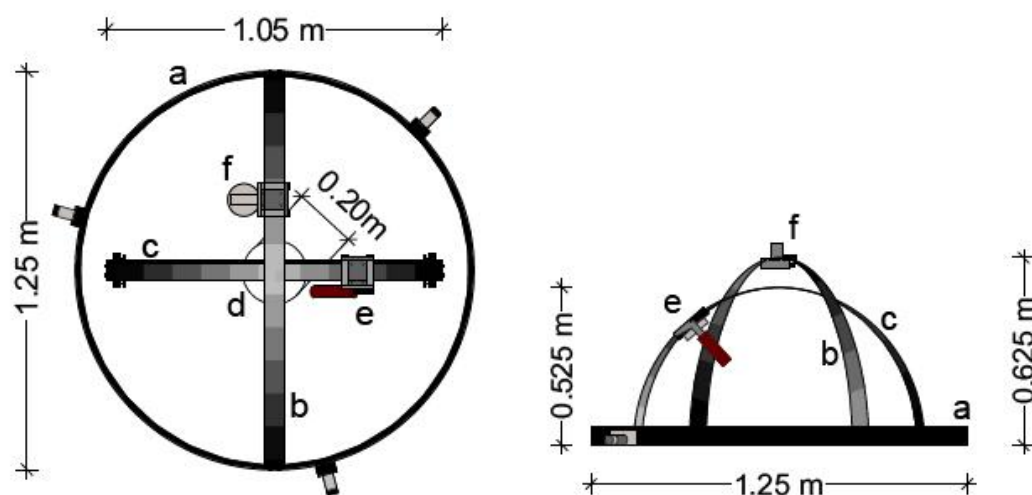
Twelve BRF cycle repetitions were acquired for each light source zenith position obtaining a full hemispherical coverage in hyperspectral mode with an angular sampling step of 30° in azimuth and 15° in zenith [26]. Under that scheme, a BRF cycle contained all possible zenith and azimuth positions of the sensor as well as the azimuth positions of the light source, 720 in total. The light source and the sensor moved in azimuthal mode, while to acquire the sensor azimuthal angular configuration the leaf sample holder rotated. In total, 60 leaves were used to account for the 12 repetitions times and the five possible zenith positions of the light source (nadir to 60°). Each cycle has a time span of less than 26 minutes to provide a minimum change in reflectance under laboratory light heat conditions in order to eliminate the drying-out effects [16]. Therefore, separate leaves were used for each zenith position of the light source.

The Bidirectional Reflectance Factor,  $R$ , is defined as the ratio of radiance reflected from a surface into a specific direction to the reference radiance,  $L_{\text{ref}}$ , reflected from an ideal lossless Lambertian reference surface measured under identical viewing and illumination geometry [27]. When the bidirectional reflectance properties of a surface are measured, the measurement procedure follows the definition of the BRF [28]. For a single direction illumination condition the BRF can be written as:

$$R(\theta_i, \phi_i; \theta_r, \phi_r; \lambda) = \frac{L(\theta_i, \phi_i; \theta_r, \phi_r; \lambda)}{L_{\text{ref}}(\theta_i, \phi_i; \theta_r, \phi_r; \lambda)} \quad (7)$$

However, under laboratory conditions, the resulted measured values produced the Biconical Reflectance Factor instead of the Bidirectional Reflectance Factor [29]. Thus a correction factor compensating the conical effect of the light source as well as the non-Lambertian reflection behavior of the Spectralon reference panel was provided [16,30].

**Figure 1.** Picture and mechanical system setup of the Compact Laboratory Spectro-Goniometer (CLabSpeG). In the horizontal plane an aluminium rail (a) supports the light source arm (b) and rotates anti-clock wise with an angular sampling step of  $30^\circ$ . A stationary arm (c) supports the hyperspectral sensor. Light source (f) and spectroradiometer (e) have an operational angular sampling step of  $15^\circ$ . In the centre there is the sample holder including a leaf (d), rotating clock-wise with an angular sampling step of  $30^\circ$  [16].



## 4. Methodology

### 4.1. Leaf variance

All 12 repetitions of BRF measurements were analyzed to investigate the differences between the individual measurements. Since all leaves were collected from the same positions, trees, and stand, it

was assumed that these leaves belonged to the same population. The Quantile-quantile (QQ) relationship was used to confirm this hypothesis.

#### 4.2. RPV inversion

The inversion of the Rahman-Pinty-Verstraete (RPV) model was performed by the RPV<sub>inversion-2</sub> software package based on BRF measurements retrieved from the goniometer [12]. This software package allowed us to perform, under the classical Bayesian approach, the inversion of the nonlinear RPV model in a numerically and computationally efficient manner. The inversion methodology aims to optimize the use of available information specified through a priori knowledge of model parameter values, the measurements, and the constraints provided by the model. Thus the RPV<sub>inversion-2</sub> software package is iteratively seeking the minimum of a cost function defined by the above information. Readers are advised to refer to the documentation of the RPV<sub>inversion-2</sub> software package for further details [12].

This procedure resulted in sets of RPV parameters and additional information including the number of iterations, the value of the cost function, and model uncertainties. The initial RPV parameters ( $\rho_0$ ,  $k$ , and  $\Theta$ ) were set at initial condition values (0.5, 0.5, and 0.5).

The BRF dataset was split into two groups: (1) eight BRF dataset repetitions were selected for the inversion procedure of the RPV model for BRF measurements at different zenith positions of the light source, ranging from 0° to 60° by steps of 15°. (2) Four datasets not included as input to the RPV<sub>inversion-2</sub> software package were used to examine the robustness of the RPV inversion through evaluation of the extracted parameters. The RPV inversion methodology was performed for each light source zenith angle ranging from 0° to 60°.

Measured and modelled data were compared using the Correlation Coefficient and the Root Mean Square Error. In addition the  $\chi^2$  method (equation 8) for a significance level  $\alpha = 0.05$  was used to evaluate the performance and the fitting of the model parameters.

$$\chi^2 = \sum \frac{(\text{measured} - \text{RPV})^2}{\text{RPV}} \quad (8)$$

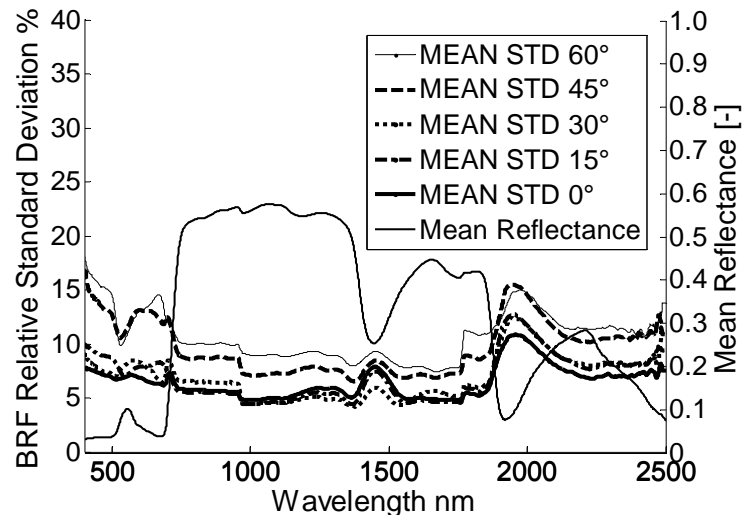
where *measured* is the laboratory measured reflectance data and *RPV* is the modelled reflectance data.

## 5. Results and Discussion

### 5.1. BRF variance

Analysis of the BRF measurements based on the Quantile-quantile (QQ) relationship confirmed that the leaves belong to the same population and distribution (results not shown). The variability in the BRF repetitions in terms of relative standard deviation (%) is highlighted in Figure 2.

**Figure 2.** Relative standard deviation in % of the mean BRF of all 12 azimuth sensor positions for sensor zenith at 0°, 15°, 30°, 45°, and 60°. The light source is at 15° zenith and 0° azimuth. The mean reflectance among the 12 azimuth sensor position is presented with a thin solid line with the reflectance values on the right scale.



The BRF databases of the current study which consisted of reflectance measurements among different *Fagus sylvatica* L. leaves agreed with the statement of [1] that the variability is less in the NIR and SWIR regions of the spectrum for the same species.

The reflectance variability of the leaves followed similar trends and patterns, thus indicating the ability to group them and statistically extract meaningful results. Specifically, higher variability was present in the visible green region, while in the infrared part of the spectrum increased variability was observable in the water absorption bands. Considering the angular effect in leaf reflectance, and thus the BRF results, it was observed that the variability, and therefore the standard deviation, is increasing with increasing viewing angles as can be seen in Figure 2.

Although, 12 azimuth positions exist for the light source, it was observed that for different goniometric measurements cycles, the variability for all azimuth positions followed the same trend as the 0° light source azimuth presented in Figure 2, exhibiting the same wavelength reflectance trend and relatively same mean, maximum and minimum values with a deviation not higher than 10.00%. In a similar fashion the variability for different sensor zenith positions follows the trends shown in Figure 2.

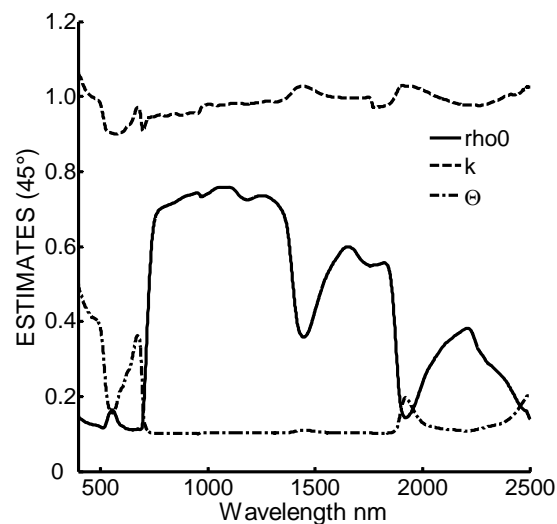
Figure 2 shows that the BRF variability of different sensor zenith positions and different leaves presented lower and more stable values in the infrared part than in the visible part of the spectrum. However, there were two profound peaks in the red region and in the water absorption region centred at 1,950 nm. The mean relative standard deviation increased with increasing light source and sensor zenith angle. At nadir, the 12 measured leaves presented the lowest variability for all wavelengths. In the NIR part of the spectrum, the variability was 6.02% while in the visible part the variability increased up to 10%. At 15° and 30° sensor zenith angles, the variability increased in the visible and especially in the red and green part of the spectrum reaching values of 15.03% and 12.12%, respectively. The same increase was present at the water band absorption at 1,950 nm. At 45° and 60° the highest variability in reflectance was observed, with values approaching and even exceeding

20.00% for the green and the red region, while the same increase was evident for the 1,950 nm region. As far as the infrared region was concerned, the variability increased with higher sensor zenith angles reaching a peak slightly higher than 10.00% for the 60° sensor zenith angle. The variability is also increasing for the water absorption band at 1,450 nm for zenith angles higher than 30°, reaching a maximum of 13.38% at the highest zenith sensor angle.

## 5.2. RPV model

Based on the RPV inversion methodology, the adjusted parameters  $\rho_0$ ,  $k$ , and  $\Theta$  for all wavelengths for light source zenith angle at 45° are presented in Figure 3.

**Figure 3.** The RPV model parameters  $\rho_0$ ,  $k$ , and  $\Theta$  for all wavelengths, are presented for the eight BRF measurements with light source at 45°.



The  $\rho_0$  parameter followed the reflectance pattern of a leaf, with maximum and minimum values of 0.75 at 1015 nm and 0.11 at 603 nm, respectively. Parameter  $k$  was close to 1 for all wavelengths, while  $\Theta$  was always positive ( $> 0$ ). The maximum, minimum and mean values of these parameters were 1.05 at 400 nm, 0.89 at 525 nm, and 0.98 for  $k$  and 0.49 at 400 nm, 0.10 at 907 nm, and 0.14 for  $\Theta$ . It was observed that the  $k$  parameter presented values greater than 1 in the water absorption bands and in the 400 nm region. This discrepancy is attributed to the higher reflectance variability among leaves, as seen in Figure 2, as well as to the possible drying effects occurring in these regions of the electromagnetic spectrum.

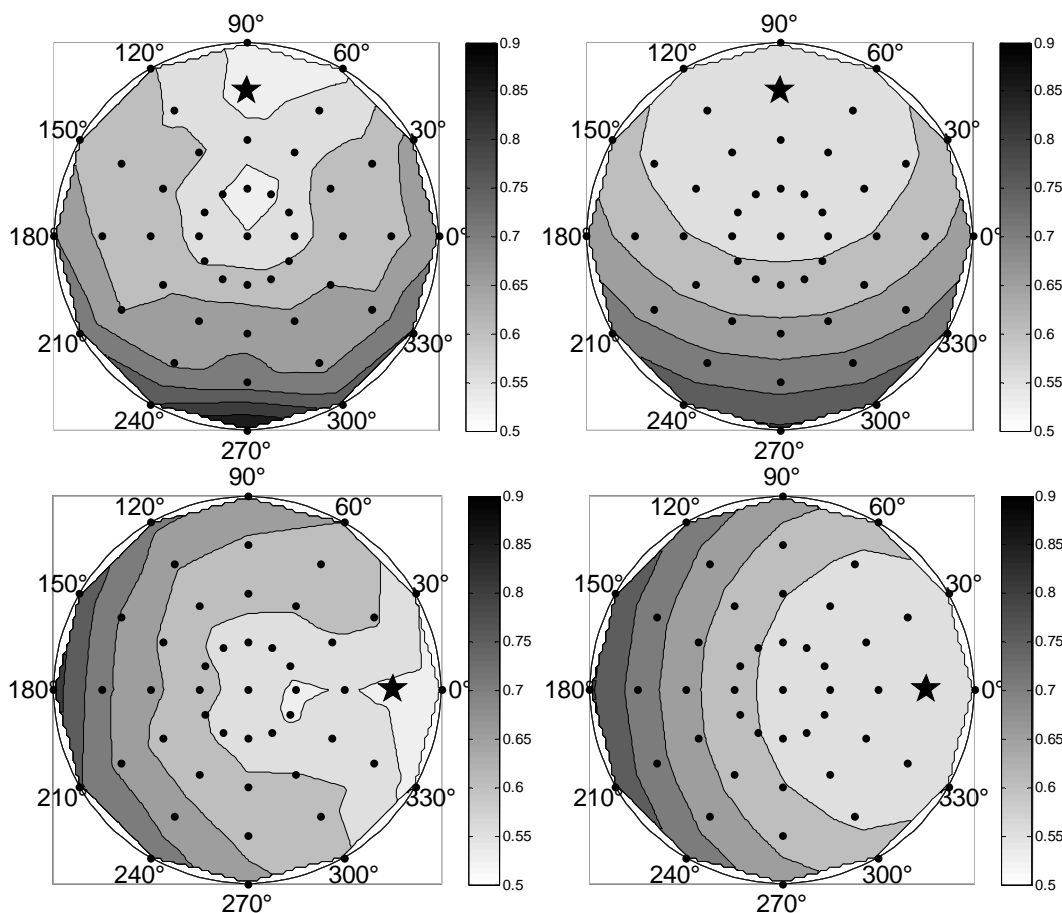
The minimum number of iterations was eight while the maximum was 30 which were determined by the gradient of the cost function used in the RPV inversion-2 software package. In the inversion process the minimization stopped once the norm of this gradient was less than a prescribed threshold value equal to  $10^{-6}$ . The estimated values of the standard deviation associated with the mean values of the retrieved parameters in the principal plane are presented in Table 1. It was observed that for higher zenith angles at 0° and 15° the estimates presented a more Lambertian behaviour with values of  $k$  closer to 1 and  $\Theta$  closer to 0. Furthermore, RPV extracted parameters are presented in table 1 for three wavelengths, namely: 550 nm, 850nm, and 1,650 nm.

**Table 1.** Mean and Standard Deviations (St. dev) of the RPV model parameters as retrieved by the inversion for three wavelengths (550 nm, 850 nm, and 1,650 nm) at zenith light source of 45°.

Viewing Conditions Principal plane	rho0		k		Θ	
	Mean	St. dev	Mean	St. dev	Mean	St. dev
550 nm	0.161	$0.83 \times 10^{-2}$	0.903	$2.43 \times 10^{-2}$	0.159	$0.43 \times 10^{-2}$
850 nm	0.718	$1.09 \times 10^{-2}$	0.954	$2.93 \times 10^{-2}$	0.101	$0.27 \times 10^{-2}$
1,650 nm	0.599	$0.99 \times 10^{-2}$	0.996	$1.38 \times 10^{-2}$	0.103	$0.36 \times 10^{-2}$

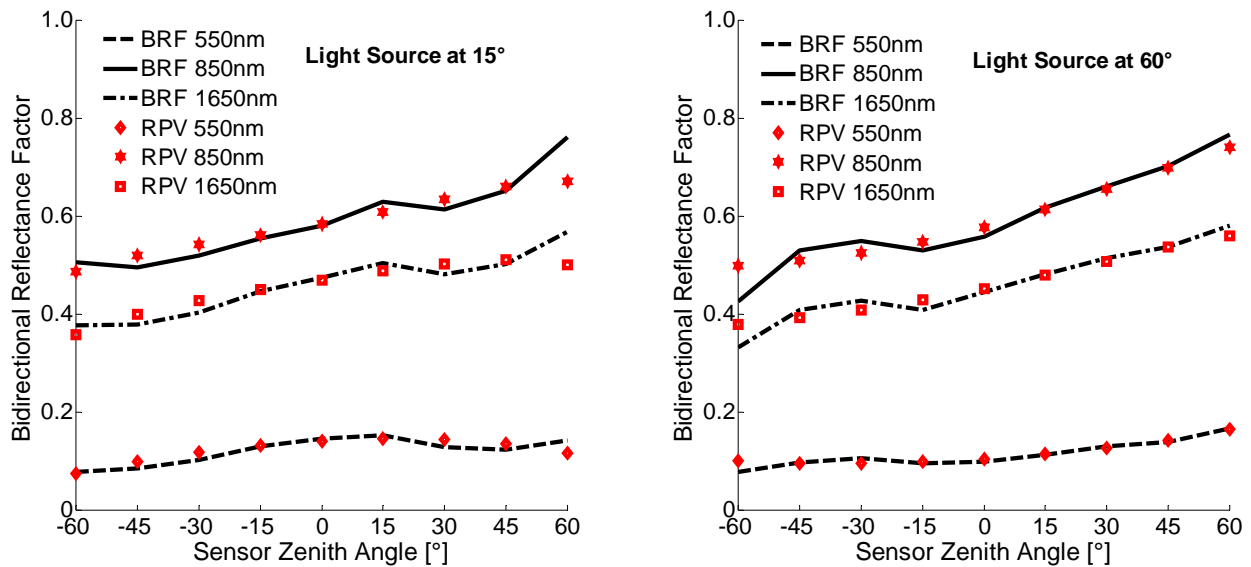
In Figure 4 the measured BRF data (left) together with the retrieved RPV (right) data are presented for two azimuth light source positions, namely 0° and 90°. The zenith light source is at 45° in both cases and the 850 nm wavelength is depicted.

**Figure 4.** Bidirectional Reflectance Factors of a *Fagus sylvatica* L. leaf at 850 nm, for light source position set at 45° zenith and 90° azimuth (top panel) and 45° zenith and 0° azimuth (bottom panel). On the right side of the Figure the simulated RPV Bidirectional Reflectance Factors are presented for the same angular and wavelength configurations. The sensor is azimuthally positioned all over the hemisphere and ranges in zenith between 0° and 60°, with 15° increments. Sensors positions are marked by dots, while incident direction is presented by a star. The bar scale indicate reflectance values.



In Figure 5 the principal plane for measured and RPV retrieved BRF values is presented for three wavelengths and two light source zenith positions. The principal plane provides a more precise estimation of the RPV set or parameter values and should be preferred when there is no limitation on the angular sampling of BRF (12).

**Figure 5.** Principal plane of the Bidirectional Reflectance Factor for measured reflectance and RPV estimations for the wavelengths of 550 nm, 850 nm, and 1,650 nm.



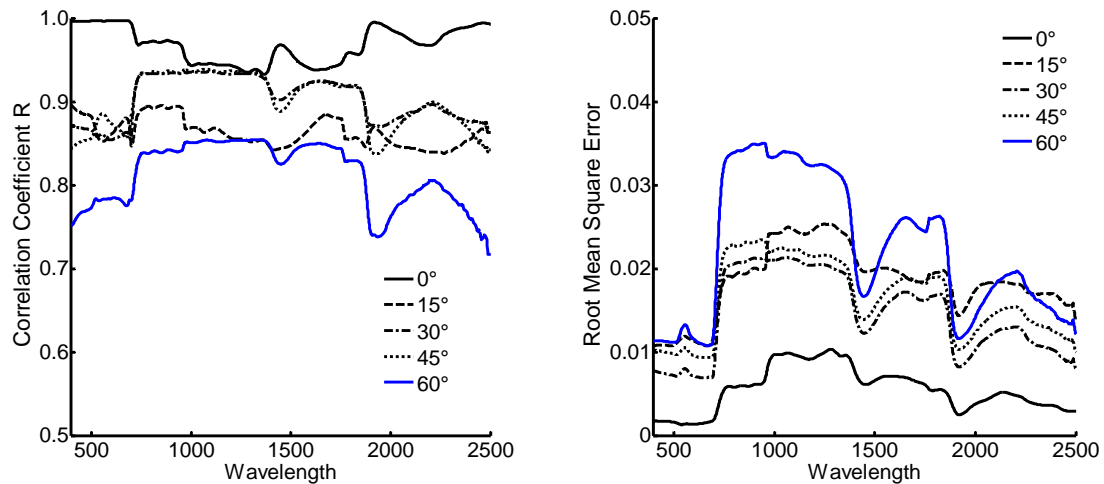
The BRF simulated by the RPV model closely matched the measured BRF values for the same light source positions and even provided the forward scattering that was observed in the leaf reflectance measurements. For these wavelengths  $\chi^2$  values are presented in Table 2.

**Table 2.**  $\chi^2$  and p values for a significance level  $\alpha = 0.05$  for three wavelengths and two light source zenith positions. The p-value for 8 degrees of freedom (9 sensor zenith positions) is 15.51.

Viewing Conditions Principal plane	Light source zenith	$\chi^2$	p-value
550 nm	15°	7.805	15.51
850 nm	15°	6.576	15.51
1,650 nm	15°	6.781	15.51
550 nm	60°	7.845	15.51
850 nm	60°	6.543	15.51
1,650 nm	60°	6.762	15.51

The good fit among the RPV model simulations and the measured data, as suggested by the  $\chi^2$ , being smaller than the p-value, demonstrates the good global model performance. The Correlation Coefficient and Root Mean Square Error for all angular combinations at light source zenith angles of 0° to 60° are given in Figure 6.

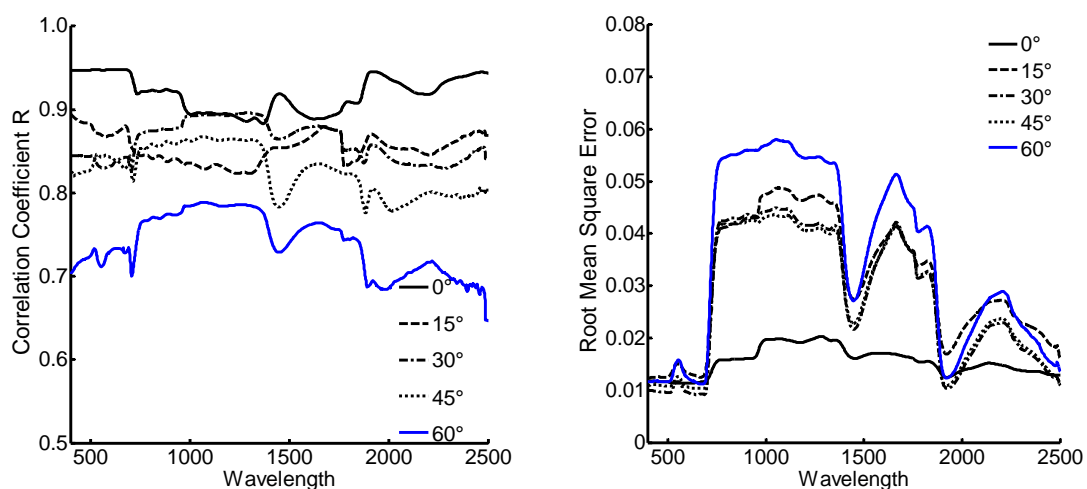
**Figure 6.** Correlation Coefficient R (left graph) and Root Mean Square Error (right graph) between measured and RPV reflectance for different light source zenith positions.



The nadir light position provides a higher correlation than higher zenith positions with values ranging between 0.94 and 0.99. These correlation differences are attributed to the fact that higher differences of the reflectance of leaves are present in higher zenith angles as seen in Figure 2. At 0° we notice the higher correlation between measurements and model simulations especially in the visible range between 400 and 700 nm while it slightly drops in the infrared region. At 15°, 30°, and 45° high Correlation Coefficients are observed for all wavelengths, while at 60°, they vary between 0.71 and 0.85. Similarly the Root Mean Square Error is higher for higher light source zenith positions.

In order to evaluate if the extracted parameters of the RPV model can simulate leaf reflectance compared with leaves other than the ones used in the inversions we calculated the Correlation Coefficient and Root Mean Square Error for the remaining set of leaves, i.e., the BRF datasets of leaves that did not participate in the inversion of RPV. Correlation Coefficient presented similar patterns although lower values compared to the leaves used in the inversion as demonstrated in Figure 7.

**Figure 7.** Correlation Coefficient R (left graph) and Root Mean Square Error (right graph) between measured data not participating in the inversion process and RPV reflectance for different light source zenith positions.



Correlation Coefficient for the leaves used for evaluation presented the higher values at 0° light source zenith position, ranging between 0.88 and 0.94, and the lower at 60° with values between 0.64 and 0.78. Overall, the agreement between modelled results and observed measurements of the evaluation data set suggests that RPV could be used to represent a generalized BRDF of *Fagus sylvatica* L. leaves for the full dynamic spectrum range.

The RPV model parameters represent the main aspects of the BRDF shape by separating it into overall brightness ( $\rho_0$ ), bowl-bell shaped anisotropy ( $k$ ), and degree of forward or backward scattering ( $\Theta$ ). If the  $k$  exponent equals one, then we have a Lambertian surface. In our case  $k$  was lower than one all over the measured wavelength revealing a “bowl-shaped” pattern. The positive values of  $\Theta$  indicate that forward scattering is dominant for all the wavelength range between 400 nm and 2,500 nm. The forward scattering was observed in other laboratory leaf BRDF measurements such as [31] and supports the results that canopy reflectance signals present a backscattering reflectance due to canopy structure effects. The global performance of the model as depicted by the Correlation Coefficient and the  $\chi^2$  demonstrated the good fitting among the RPV model and the measured data.

## 6. Conclusions and Recommendations

The inversion of the widely applied Rahman-Pinty-Verstraete (RPV) model based on Bidirectional Reflectance Factor (BRF) data sets of *Fagus sylvatica* L leaves in the 400 to 2,500 nm spectral range was presented. These BRF data sets were collected using the CLabSpeG laboratory goniometer. A statistical analysis on the BRF variability of different leaves from the same tree showed that leaf reflectance among the same specie presents a higher variability in the visible domain, apart from the green region, than in the infrared part of the spectrum. This variability increases with increasing zenith angles.

The RPV model parameters were retrieved for all light/sensor angular positions and the Correlation Coefficient of measured and RPV generated BRFs varied between 0.71 and 0.99 for all wavelengths and azimuth and zenith positions. Although no previous research is known in inverting the RPV model for leaf elements, our RMSE and Correlation Coefficient are in agreement with the model performance for green grass measured in laboratory conditions and alfalfa measured outdoors [2,32]. Moreover, the  $\chi^2$  values indicated that the RPV provides a good fitting to our measured data. The simulated RPV model values were compared with an independent set of measurements and also presented an adequate Correlation Coefficient. Contrary to canopy reflectance measurements [13,15], our results presented the strongest anisotropy in the forward scattering direction indicating the importance and the dominant role of canopy architecture in the total reflectance signal of a scene. Higher correlations were found in lower zenith angles and especially at nadir position. It should be noted that the measured BRF values might be affected, especially in the water absorption bands, from the time and heating stress due to the measurement procedure of the goniometer. Under the measurement time of 26 minutes there were changes in the water absorption band of up to 15% [16]. Conclusively, we presented that a semi empirical model typically used for simulating canopy reflectance could also be used for simulating individual canopy elements such as leaves and it could be used as BRDF input parameter in a number of applications oriented either to simulation, modelling or visualization.

## Acknowledgements

We would like to thank Dr. Marco Clerici from Joint Research Centre for his support and suggestions regarding the RPV inversion-2 software.

## References and Notes

1. Asner, G.P. Biophysical and biochemical sources of variability in canopy reflectance. *Remote Sens. Environ.* **1998**, *64*, 234-253.
2. Boucher, Y.; Cosnefroy, H.; Petit, D.; Serrot, G.; Briottet, X. Comparison of measured and modeled BRDF of natural targets. *N° 3699-02 SPIE AeroSense*, Orlando, FL, USA, April, 1999; pp. 16-26.
3. Maignan, F.; Bréon, F.M.; Lacaze, R. Bidirectional reflectance of earth targets, evaluation of analytical models using a large set of spaceborne measurements with emphasis on the hot spot. *Remote Sens. Environ.* **2004**, *90*, 210-220.
4. Schönemark, M.; Geiger, B.; Röser, H.P. *Reflection Properties of Vegetation and Soil with a BRDF Data base*. Wissenschaft und Technik Verlag: Berlin, Germany, 2004; p. 352.
5. Roujean, J.-L.; Leroy, M.; Deschamps, P.Y. A bi-directional reflectance model of the Earth's surface for the correction of remote sensing data. *J. Geophys. Res.* **1992**, *97*, 20455-20468.
6. Rahman, H.; Verstraete, M.M.; Pinty, B. Coupled Surface-Atmosphere Reflectance (CSAR) model 1. Mmodel description and inversion on synthetic data. *J. Geophys. Res.* **1993**, *98*, 20779-20789.
7. Rahman, H.; Pinty, B.; Verstraete, M.M. Coupled Surface-Atmosphere Reflectance (CSAR) model 2. Semiempirical surface model usable with noaa advanced very high resolution radiometer data. *J. Geophys. Res.* **1993**, *98*, 20791-20781.
8. Pinty, B.; Widlowski, J.-L.; Taberner, M.; Gobron, N.; Verstraete, M.M.; Disney, M.; Gascon, F.; Gastellu, J.-P.; Jiang, L.; Kuusk, A.; Lewis, P.; Li, X.; Ni-Meister, W.; Nilson, T.; North, P.; Qin, W.; Su, L.; Tang, S.; Thompson, R.; Verhoef, W.; Wang, H.; Wang, J.; Yan, G.; Zang, H. Radiation Transfer Model Intercomparison (RAMI) exercise, results from the second phase. *J. Geophys. Res.* **2004**, *109*, D06210, doi:10.1029/(2003)JD004252.
9. Widlowski, J.-L.; Taberner, M.; Pinty, B.; Bruniquel-Pinel, V.; Disney, M.; Fernandes, R.; Gastellu-Etchegorry, J.-P.; Gobron, N.; Kuusk, A.; Lavergne, T.; Leblanc, S.; Lewis, P.E.; Martin, E.; Möttus, M.; North, P.R.J.; Qin, W.; Robustelli, M.; Rochdi, N.; Ruiloba, R.; Soler, C.; Thompson, R.; Verhoef, W.; Verstraete, M.M.; Xie, D. Third Radiation Transfer Model Intercomparison (RAMI) exercise: Documenting progress in canopy reflectance modeling. *J. Geophys. Res.* **2007**, *112*, D09111, doi:10.1029/(2006)JD007821.
10. Zhang, Z.; Kalluri, S.; JaJa, J.; Liang, S.; Townshend, J.R.G. High performance algorithms for global BRDF retrieval. *IEEE Comput. Sci. Eng.* **1998**, *4*, 16-29.
11. Gobron, N.; Lajas, D. A new inversion scheme for the RPV model. *Can. J. Remote Sens.* **2002**, *28*, 156-167.

12. Lavergne, T.; Kaminski, T.; Pinty, B.; Taberner, M.; Gobron, N.; Verstraete, M.M.; Vossbeck, V.; Widlowski, J.-L.; Giering, R. Application to MISR land products of an RPV model inversion package using adjoint and Hessian codes. *Remote Sens. Environ.* **2007**, *107*, 362-375.
13. Li, X.; Strahler, A.H. Geometrical - optical modelling of a conifer forest canopy. *IEEE Trans. Geosci. Remote Sens.* **1985**, *23*, 705-721.
14. Walter-Shea, E.A.; Norman, J.M.; Blad, B.L. Leaf bidirectional reflectance and transmittance in corn and soybean. *Remote Sens. Environ.* **1989**, *29*, 161-174.
15. Pinty, B.; Verstraete, M.M.; Gobron, N. The effect of soil anisotropy on the radiance field emerging from vegetation canopies. *Geophys. Res. Lett.* **1998**, *25*, 797-800.
16. Biliouris, D.; Verstraeten, W.W.; Dutré, P.; Aardt, J.A.N.; Muys, B.; Coppin, P. A Compact Laboratory Spectro-Goniometer (CLabSpeG) to assess the BRDF of materials. Presentation, calibration and implementation on *Fagus sylvatica* L. leaves. *Sensors* **2007**, *7*, 1846-1870.
17. Verstraete, M.M.; Pinty, B.; Myneni, R.B. Potential and limitations of information extraction on the terrestrial biosphere from satellite remote sensing. *Remote Sens. Environ.* **1996**, *58*, 201-215.
18. Martonchik, J.V.; Diner, D.J.; Kahn, R.A.; Ackerman, T.P.; Verstraete, M.M.; Pinty, B.; Gordon, H.R. Techniques for retrieval of aerosol properties over land and ocean using multiangle imaging. *IEEE Trans. Geosci. Remote Sens.* **1998**, *36*, 1212-1227.
19. Lattanzio, A.; Govaerts, Y.M.; Pinty, B. Consistency of surface anisotropy characterization with meteosat observations. *Adv. Space Res.* **2007**, *39*, 131-135.
20. Schaaf, C.B.; Gao, F.; Strahler, A.H.; Lucht, W.; Li, X.; Tsang, T. First operational BRDF, albedo and nadir reflectance products from MODIS. *Remote Sens. Environ.* **2002**, *83*, 135-148.
21. Widlowski, J.-L.; Pinty, B.; Gobron, N.; Verstraete, M.M.; Davies, A.B. Characterization of surface heterogeneity detected at the MISR/TERRA subpixel scale. *Geophys. Res. Lett.* **2001**, *28*, 4639-4642.
22. Gao, F.; Schaaf, C.B.; Strahler, A.H.; Jin, Y.; Li, X. Detecting vegetation structure using a kernel-based BRDF model. *Remote Sens. Environ.* **2003**, *86*, 198-205.
23. Engelsen, O.; Pinty, B.; Verstraete, M.M.; Martonchik, J.V. Parametric bidirectional reflectance factor models: evaluation, improvements and applications. *Catalogue CL-NA-16426-EN-C, ECSC-EC-EAEC*. Brussels, Luxembourg, 1996; p.114.
24. Minnaert, M. The reciprocity principle in lunar photometry. *Astrophys. J.* **1941**, *93*, 403-410.
25. Henyey, L.G.; Greenstein, T.L. Diffuse radiation in the galaxy. *Astrophys. J.* **1941**, *93*, 70-83.
26. Sandmeier, St. Acquisition of bidirectional reflectance factor data with field goniometers. *Remote Sens. Environ.* **2000**, *73*, 257-269.
27. Nicodemus, F.E.; Richmond, J.C.; Hsia, J.J.; Ginsberg, I.W.; Limperis, T. Geometrical considerations and nomenclature for reflectance, *National Bureau Standards Monograph*, Inst. for Basic Standards: Washington, DC. USA, 1977; p. 160.
28. Martonchik, J.V.; Bruegge, C.J.; Strahler, A.H. A review of reflectance nomenclature used in remote sensing. *Remote Sens. Rev.* **2000**, *19*, 9-20.
29. Schaepman-Strub, G.; Schaepman, M.E.; Painter, T.H.; Dangel, S.; Martonchik, J.V. Reflectance quantities in optical remote sensing -definitions and case studies. *Remote Sens. Environ.* **2006**, *103*, 27-42.

30. Dangel, S.; Verstraete, M.M.; Schopfer, J.; Kneubuhler, M.; Schaepman, M.; Itten, K.I. Toward a direct comparison of field and laboratory goniometer measurements. *IEEE Trans. Geosci. Remote Sens.* **2005**, *43*, 2666-2675.
31. Bousquet, L.; Lachérade, S.; Jacquemoud, S.; Moya, I. Leaf BRDF measurements and model for specular and diffuse components differentiation. *Remote Sens. Environ.* **2005**, *98*, 201-211.
32. Boucher, Y. Analyzing some models for a given type of surface. In *Reflection Properties of Vegetation and Soil with a BRDF Data base*. Schönemark, M., Geiger, B., Röser, H.P., Eds.; Wissenschaft und Technik Verlag: Berlin, Germany, 2004; pp. 121-129.

© 2009 by the authors; licensee Molecular Diversity Preservation International, Basel, Switzerland. This article is an open-access article distributed under the terms and conditions of the Creative Commons Attribution license (<http://creativecommons.org/licenses/by/3.0/>).